

Effects of flow and dissipation on acoustical behavior of complex cavities

Y. Aurégan and V. Pagneux

Laboratoire d'Acoustique de l'Université du Maine, UMR CNRS 6613

Av. O Messiaen, 72085 LE MANS Cedex 9, France

This work is dedicated to the experimental analysis of the statistics of the scattering of sound in a complex cavity. The tools, developed in other context, and especially the Random Matrix Theory can explain very well the statistics of those cavities. An emphasis is made in this study to the effect of dissipation and of flow on the cavity statistics.

I. Introduction

In the airflow system of many industrial applications, large enclosures connected to ducts or complex duct networks can be found. In the aeronautical industry, a typical example is the air conditioning distribution system of an aircraft. From the acoustical point of view, these systems have a size much larger than the wavelength and an irregular geometry.

In the limit where the wavelength is small compared to the characteristic size of the enclosures, wave propagation inside the enclosure can be modeled using ray trajectories. If the geometry is irregular and in the limit of very short wavelength, those wave systems can exhibit ray chaotic properties. This wave chaos has been intensively studied in the context of quantum mechanical waves,¹ however, the concepts that have been developed can generally be extended to classical waves^{2,3} In particular, Random Matrix Theory (RMT) was shown to be an efficient tool to obtain results on the distribution of transmission and reflection coefficients (e.g. Schanze *et al.*⁴ and Hemmady *et al.*⁵).

The idea behind the Random Matrix Theory of scattering is to assume that the dynamics of the wave is so irregular that it implies random distribution of the scattering coefficients. Then it remains to define the probability density of the scattering matrix; it is obtained by keeping only the fundamental properties of the propagation, i.e. the conservation of energy and/or the reciprocity. For instance, by keeping only the conservation of energy, the scattering matrix has to be unitary and the probability density is chosen as the uniform distribution on the compact set of unitary matrices.⁶ The introduction of damping is also possible by suitable modeling of the attenuation.⁷

Of course, acousticians rarely encounter truly lossless systems in practice. Furthermore, in duct systems the flow is very often present. Thus in this paper, we explore experimentally a generic cavity in which we control both the flow and the dissipation. We compare these experimental results with results predicted by RMT.

II. Experimental setup

The cavity is a parallelepipedic box of $0.924 \times 0.962 \times 0.565$ m³. The box is made of wood plates (thickness 20 mm) and some stiffeners are screwed and glued on the external faces to avoid, as much as possible, sound losses through the box enclosure. A cylinder of diameter 0.2 m, half a cylinder, and two quarter of cylinder has been added in the box to break all its symmetries (See Fig. 1) and to insure a chaotic behavior of rays in this box. The position of the vertical cylinder can be changed to ensure various realizations of the chaotic acoustical field.

Porous material can be inserted in the box to control volume dissipation. This porous material is a melamine foam (panels of 300 mm \times 200 mm \times 50 mm). The panels are sustained by deformable rods that allow a variable orientation of the panels (See Fig. 2(a)). These panels can also be glued on one side of the

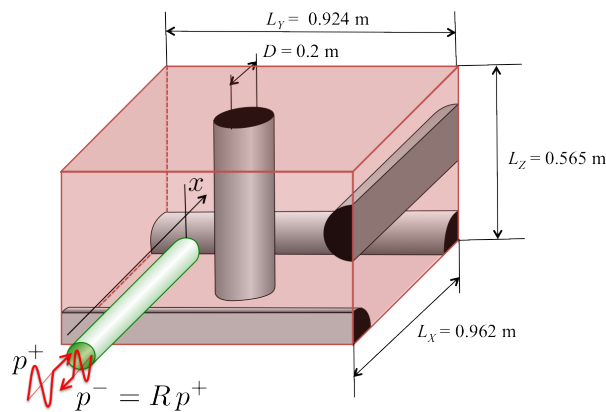


Figure 1. Geometry of the chaotic box (CB) connected to the rigid duct

box.

A flow can be produced inside this chaotic box (CB) by an internal ventilation fan (See Fig. 2(b)). This fan can provide a flow rate of $350 \text{ m}^3/\text{h}$ and has a diameter of 150 mm. The velocity at the fan exit is 5.5 m/s (1.6 % of the sound velocity). The mean velocity field in the CB is complex and has to be measured.

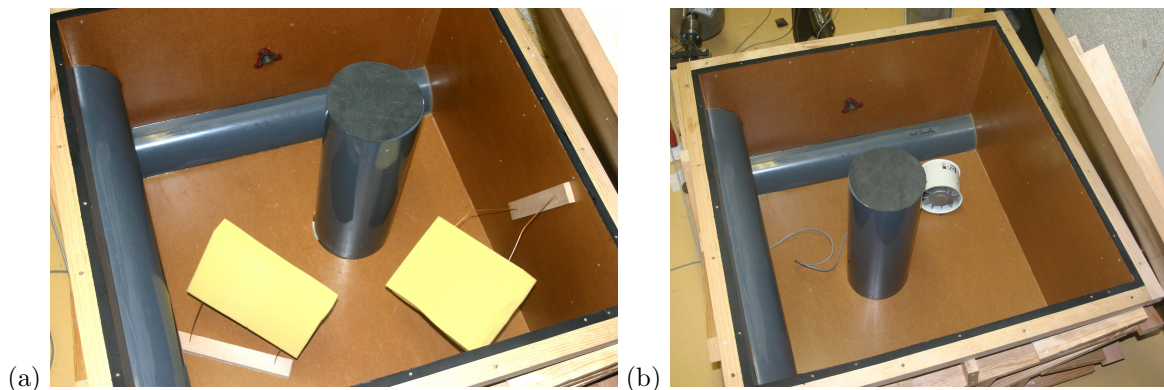


Figure 2. Photographies of the chaotic box (CB) with two porous plates (a) and with the ventilation fan (b).

The reflection coefficient of CB is measured in a duct, with microphones, attached on one side of CB. This duct (made in steel) has an inner diameter of 30mm and a thickness of 4 mm. In the frequency range of interest (0–4000 Hz), only plane wave can propagate in the duct.

The reflection coefficient R is linked to the transfer function H_{21} between the microphone 2 and 2 by

$$R = \frac{p^-}{p^+} = \frac{H_{21}e^{-jkx_1} - e^{-jkx_2}}{e^{jkx_1} - H_{21}e^{jkx_2}}$$

where $k = \omega/c_0$ is the wave number, $x_{1,2}$ are the position of the microphones 1, 2 relatively to the end of the duct. Thus, from the measurement of H_{21} , R can be known.⁸ The distance between the microphones and the box entrance is $x_1 = -0.438\text{m}$, $x_2 = -0.468\text{m}$.

III. Reflection coefficient of the cavities

The absolute value of the reflection coefficient R measured for the CB is depicted in Fig. 3. It can be observed on this figure, that the reflection coefficient has a mean part and a fluctuating part. The mean part corresponds to the radiation impedance of a tube in the CB. It can be approximated by the radiation

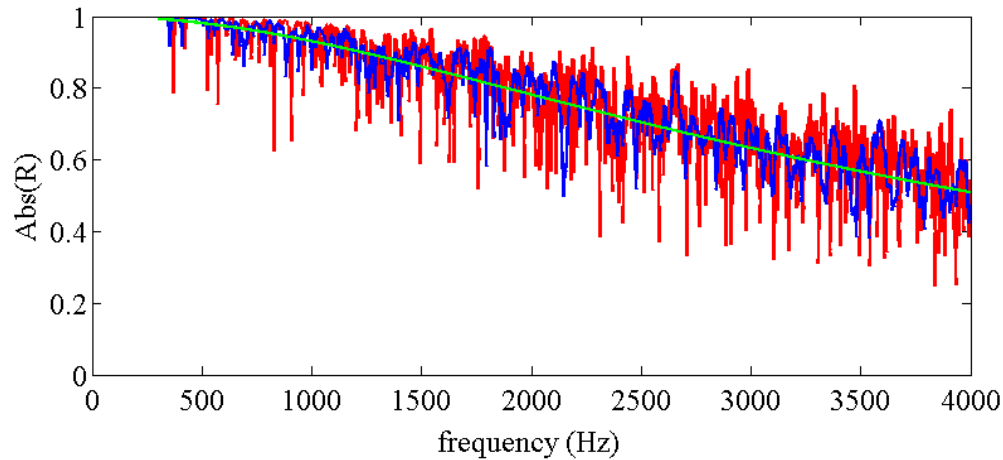


Figure 3. Experimental absolute values of the reflection coefficient of the chaotic box (CB). Red continuous: Cavity without porous; Blue continuous: Cavity with two porous panels; Green line: Theoretical radiation coefficient computed for a tube radiating in an semi-infinite space

impedance of a tube in a semi-infinite space (green line in Fig. 3) which is given by

$$Z_{rad} = 1 - \frac{J_1(2ka)}{ka} + j \frac{S_1(2ka)}{ka} \quad (1)$$

where $k = \omega/c_0$ is the wave number, a is the radius of the tube, J_1 is the order 1 Bessel function of the first kind and S_1 is the order 1 Struve function.

The fluctuating part, corresponding to the chaotic behavior of this box is superimposed to this mean part. The radiation impedance Z_{rad} takes into account the imperfect coupling between the field within the chaotic cavity and the incoming and outgoing waves in the connected tube. By suitably accounting for this coupling details, it was hoped that only universal properties of the chaotic cavity remained.

However, there may exist acoustical rays that leave the tube and soon return to it. Those short ray trajectories lead to non-universal contributions. Yeh *et al.*⁹ propose to take into account this effect by a frequency average of single-realization data. This frequency smoothing suppresses the impedance fluctuations due to long trajectories and reveals the features associated with short trajectories. The smoothing is made by convoluting the experimental results with a Hanning window of bandwidth Δf of 60 Hz. This limits the study to the trajectories with the path length $L < c_0/\Delta f \simeq 6$ m. Figure 4 shows the measured impedance, the radiation impedance and the smoothed measured impedance.

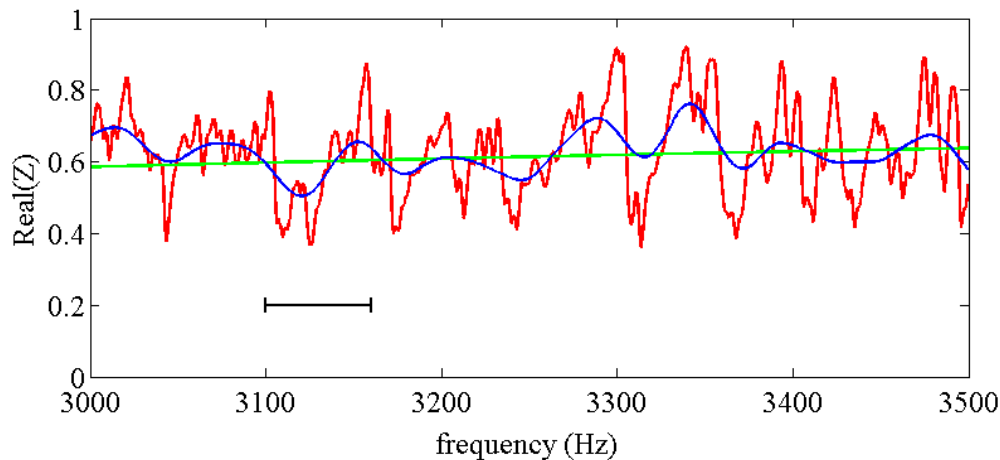


Figure 4. Real value of the measured impedance Z in red. Real value of the radiation impedance Z_{rad} in green. Real value of the smoothed impedance Z_{avg} in blue. The black interval gives the length of the smoothing window

The normalized impedance ζ can be found from the entrance impedance of the cavity Z by:⁹

$$Z = \text{Re}(Z_{avg})j\zeta + j\text{Im}(Z_{avg}) \quad \text{where} \quad Z = \frac{1+R}{1-R}. \quad (2)$$

The variance of this normalized impedance ζ is linked to the loss parameter α by $\alpha = 1/(\pi \text{ Variance})$. By measuring the variance on a sliding window of 500 Hz, the variation of the loss parameter as a function of the frequency can be computed and is shown on Fig. 5. It can be seen that the value of the variance of the real and of the imaginary part are equal, in accordance to the theory. The loss parameter α increases with frequency and the statistics had to be computed on windows where α is almost constant and that contains enough points to have a good convergence of the statistics. In the following, a window of 500 Hz with 1000 samples is chosen and 3 realizations are done by moving the cylinder, thus the statistics are made with 3000 points.

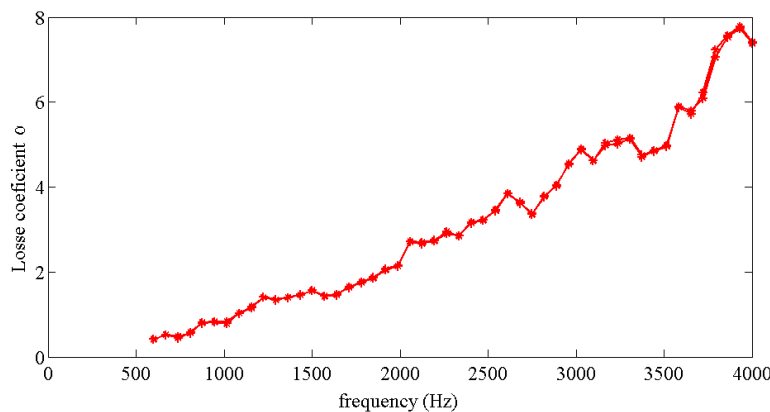


Figure 5. Loss parameter α as a function of the frequency obtaining by computing the variance of the real and the imaginary part of the normalized impedance ζ . The variance is computed on a sliding window of 500 Hz.

The probability density function (PDF) of the normalized impedance ζ for the frequency band 3000–3500 Hz is given in Fig. 6 for the empty box. On this Figure, the experimental results are compared with the RMT results with a loss parameter $\alpha = 4.15$ which is the only fit parameter for PDF of the real and the imaginary parts of ζ . The experimental results are in very good accordance with the RMT results. The value of the loss parameter indicates that there is some losses in the empty box even if some efforts have

been made to minimize them. The reverberation time (the time for a decreasing of the field by 60 dB) of this box is 0.74 s. The main dissipation process is supposed to be the coupling of the interior acoustical field with small vibrations of the walls.

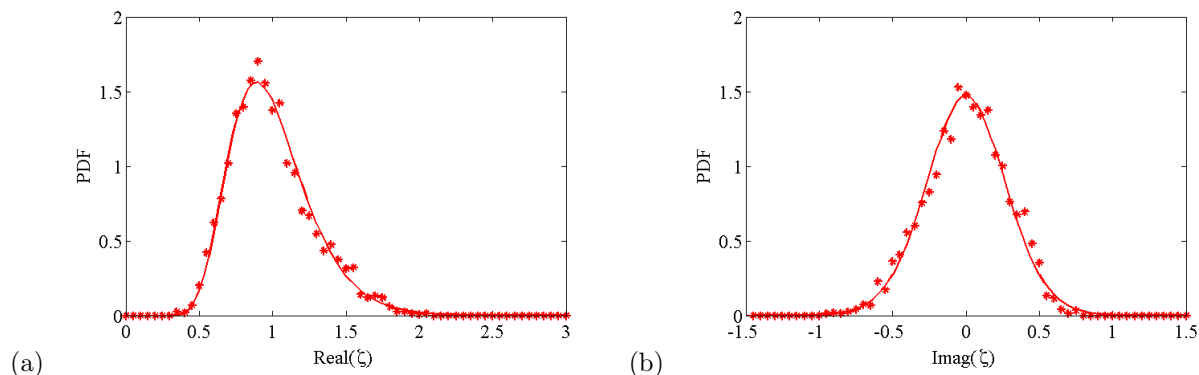


Figure 6. Probability density function of ζ for CB on the frequency band 3000–3500 Hz. (a) Real part of ζ , (b) Imaginary part of ζ . Red symbols: measurements, red line: RMT results.

IV. Effect of flow

A ventilation fan is introduced in the Chaotic Box to induce a circulation of the air in the box. The main effect of the mean flow in the box is to break the time reversal symmetry.⁴ In this case, the statistics of the impedance without time reversal symmetry is changed compared to the impedance with time reversal symmetry.

To test the repeatability of the measurements with flow, two measurements without flow and two measurements with flow have been done at different times. The results are depicted on Fig. 7. The two measurements without flow are in red and magenta and the two measurements with flow are in blue and cyan. It can be seen that the measurement are repeatable and that the flow effect is weak but observable despite its very weak value (The maximum Mach number in the box is $M = 0.016$).

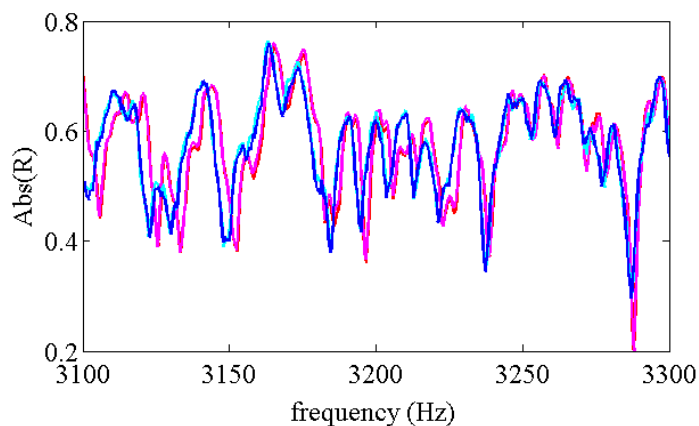


Figure 7. Absolute value of the reflection coefficient R with and without flow. The two measurements without flow are in red and magenta and the two measurements with flow are in blue and cyan.

On Fig. 8, the experimental values of the PDF of ζ is plotted without flow (red symbols) and with flow (blue symbols). There is a small but systematic deviation of the results with flow compared to the results without flow. The RMT results when time reversal symmetry is broken¹⁰ ($\alpha = 4.15$) have the same tendencies: higher and sharper peak with flow. Again the results with flow are in good accordance with the RMT results. A higher flow rate had to be tested to see if the results are closer to the values of the RMT

when time reversal symmetry is broken.

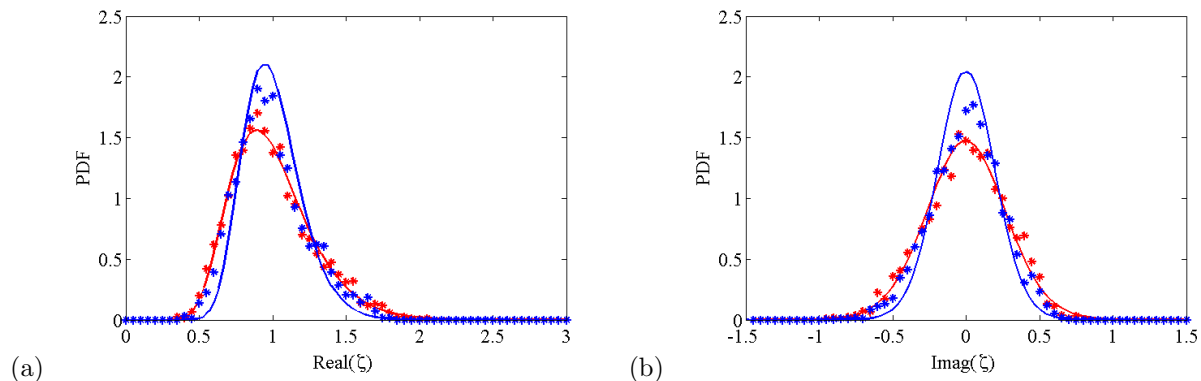


Figure 8. Probability density function of ζ for CB with and without flow on the frequency band 3000–3500 Hz. (a) Real part of ζ , (b) Imaginary part of ζ . Red symbols: measurements without flow. Blue symbols: measurements with flow, red lines: RMT results with time reversal symmetry, blue lines: RMT results without time reversal symmetry.

V. Effect of absorbing porous material

To test the effect of absorption, porous panels are introduced in the box. It can be seen in Fig. 2(a) that those panels are putting inside the volume. The main expected effect is to change the wave number k by introducing a complex part in it. The boundary conditions on the wall of the box is supposed to be unchanged.

The effects of increasing the absorption can be seen in Fig. 9: The amplitude of the fluctuating part is decreasing when the absorption increases. With higher absorption, the resonances are smoother and the number of visible resonance decreases (the mean-spacing of the adjacent resonances increases).

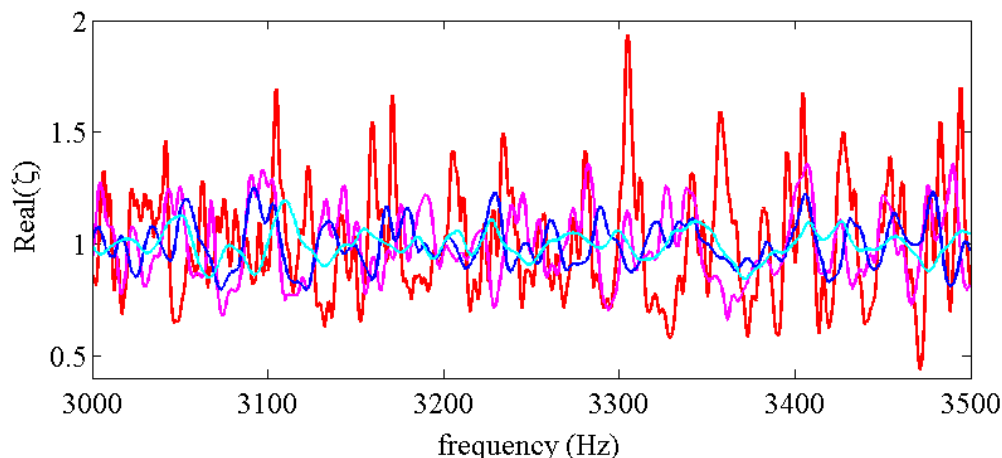


Figure 9. Real value of the normalized impedance ζ with porous panels. Red empty box, magenta: 1 panel, blue: 2 panels, cyan: 3 panels

The variation of the loss parameter as a function of the frequency for the 3 cases with porous panels can be seen on Fig. 10. The loss parameter α increases with the number of porous panels and with frequency.

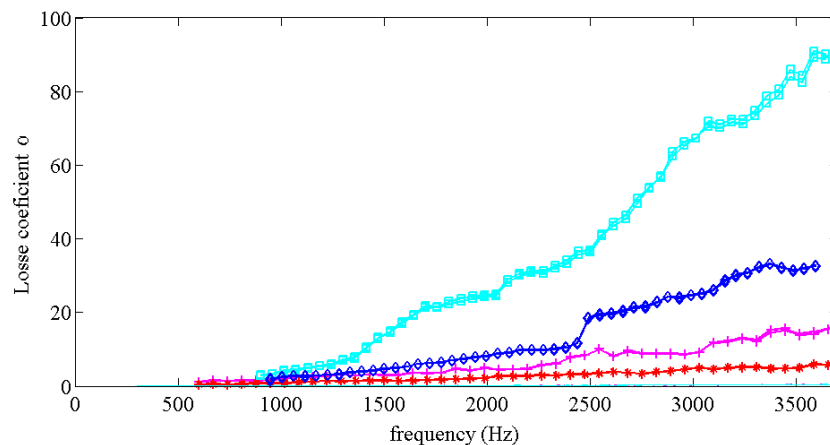


Figure 10. Loss parameter α as a function of the frequency for the empty box (red symbols) and for the box with panels of porous material (magenta symbols: 1 panel, blue symbols: 2 panels, cyan symbols: 3 panels)

On Fig. 11, the experimental values of the PDF of ζ is plotted for the 3 cases with porous panels. The experimental values (symbols) are compared to the RMT values (lines) with $\alpha=4.15$, 15.3, 31.8 and 70.7. The agreement between experimental and RMT results is good.

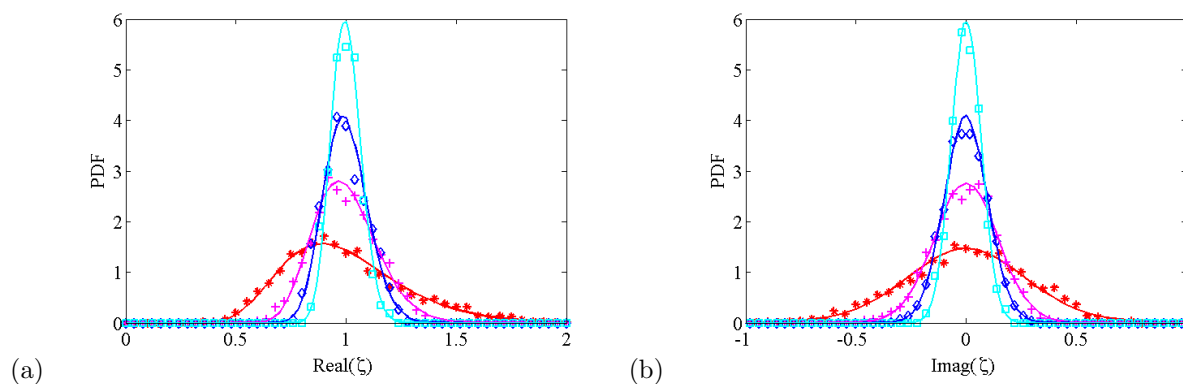


Figure 11. Probability density function of ζ for CB with and without flow and with porous materials on the frequency band 3000–3500 Hz. (a) Real part of ζ , (b) Imaginary part of ζ . Red symbols: measurements without flow. Green symbols: measurements with flow, blue symbols: measurements with 2 plates of porous material. The lines correspond to the RMT results with $\alpha=4.15$ (red), $\alpha=15.3$ (magenta), $\alpha=31.8$ (blue), $\alpha=70.7$ (cyan).

VI. Conclusion

Experiments has be conducted to measure the acoustical reflection coefficient of a box which can exhibit ray chaotic properties. We have verified that the normalized cavity impedance describes universal properties of the reflection fluctuations by properly taking into account the coupling process between the measurement duct and the cavity. The normalized impedance can be obtained by a mix of ensemble averages on various realizations and of frequency averages over bandwidth containing several oscillations. The results show that the direct processes (short ray trajectories) had to be removed to obtain converged statistics. The random matrix theory (RMT) provides a good description of the one-port wave chaotic system The reflection fluctuation statistics depend only on a single control parameter characterizing the cavity loss in the realm of intermediate to high losses induced by porous material inside the box. The breaking of the time reversal symmetry by a small airflow inside the box is also successfully described by the RMT.

Acknowledgments

The authors are grateful to Hans-Jürgen Stöckmann and Steven Anlage for helpful discussions and to Steven Anlage for providing a Matlab code to compute the RMT results with time reversal symmetry.

References

- ¹H.-J. Stöckmann, *Quantum Chaos - An Introduction* (University Press Cambridge, 1999).
- ²M. Wright and R. Weaver, *New Directions in Linear Acoustics and Vibration* (University Press Cambridge, 2010.).
- ³O. Legrand and D. Sornette, *Quantum chaos and Sabines law of reverberation in ergodic rooms* Lect. Notes Phys. 392, 267274 (1991).
- ⁴H. Schanze, H.-J. Stöckmann, M. Martínez-Mares and C.H. Lewenkopf *Universal transport properties of open microwave cavities with and without time-reversal symmetry*, Phys.Rev. E 71016223 (2005).
- ⁵S. Hemmady, X. Zheng, E. Ott, T.M. Antonsen, S.M. Anlage, *Universal impedance fluctuations in wave chaotic systems*, Phys. Rev. Lett. 94, 014102 (2005).
- ⁶M.L. Mehta, *Random Matrices*, Academic Press, New York (1991).
- ⁷P. A. Mello and N. Kumar *Quantum Transport in Mesoscopic Systems. Complexity and statistical fluctuations* Oxford University Press (2004)
- ⁸J. Y. Chung and D. A. Blaser, *Transfer function method of measuring in-duct acoustic properties. I. Theory*, J. Acoust. Soc. Am. 68, 907913 (1980).
- ⁹J.-H. Yeh, J. A. Hart, E. Bradshaw, T. M. Antonsen, E. Ott, and S. M. Anlage, *Universal and nonuniversal properties of wave-chaotic scattering systems*, Phys. Rev. E 81, 025201(R) (2010).
- ¹⁰P. W. Brouwer and C. W. J. Beenakker, *Voltage-probe and imaginary-potential models for dephasing in a chaotic quantum dot*, Phys. Rev. B 55, 4695 (1997).